Structure and Short Timescale Ion Dynamics of Potassium-Ammonia Graphite Intercalation Compounds

Leonardo Bernasconi and Paul A. Madden*

Physical and Theoretical Chemistry Laboratory, Oxford University, South Parks Road, Oxford OX1 3QZ, U.K.

Received: June 27, 2001; In Final Form: October 30, 2001

We present Generalized Gradient Corrected Density Functional Theory (DFT) calculations of the static and dynamic properties of stage-I potassium and potassium-ammonia graphite intercalation compounds KC_8 and $KC_{24}(NH_3)_x$, with $x = 0$, 1, 2, 3, 4, 4.5, 5. For each system, a full geometry optimization was carried out, and finite temperature first-principle molecular dynamics (FPMD) simulations were performed on a selected number of compounds (KC_8, KC_{24}, $KC_{24}(NH_3)_4$, and $KC_{24}(NH_3)_5$) in the temperature range 373−573 K and overall simulation times of 2−4 ps. K was found to adsorb preferentially above C_6 rings and, typically, to diffuse parallel to the *ab*-plane at finite temperature. In addition, a slow oscillatory motion perpendicular to the carbon layers was observed, with K residing in turn closer to one or another carbon plane. We speculate on these findings in their connection with the electronic properties of potassium-ammonia intercalates in the vicinity of the metal−nonmetal transition at $x \simeq 4.3$.

I. Introduction

The large spacing between parallel carbon planes of graphite and the weak interlayer bonding account for the ready cleavage along the basal plane and the remarkable softness of the crystal, and are responsible for the ability of graphite to intercalate a wide range of substances under mild conditions, to give lamellar compounds of variable composition. These reactions are often reversible and the nature of the host lattice is retained.[1] Intercalation results in a macroscopic expansion along the *c*-axis (perpendicular to the carbon planes) with respect to pure graphite, while the internal structure of the carbon layers is essentially unchanged.

Binary alkali metal graphite intercalation compounds (GICs) exist in different stages, depending on the metal concentration: MC_8 (corresponding to the highest metal concentration), MC_{24}, MC_{36}, MC_{48}, and MC_{60}, with M = K, Rb, or Cs. Pure staging is characterized by periodic stacking of intercalant layers, repeating over extended distances (>500 Å). Starting from graphite, in which the C layers are stacked in the sequence ...ABAB... with a repeat distance A−B of 3.35 Å, stage-I compounds can be formed by replacing each B plane with a plane of alkali metal, yielding a repeat pattern along the *c*-axis ...AMA... and a repeat distance I_c which is larger than the A−B separation in graphite (e.g., in KC_8, $I_c = 5.41$ Å). Further stages are characterized by different vertical stackings of the A, B, and M planes (e.g., stage-II MC_{24} has a repeated pattern ...AMABMBA..., stage-III MC_{36} ...AMABA..., and so on). Thus pure stage-*n* is characterized by a periodic arrangement in which each two successive intercalant layers at a vertical distance I_c are separated by *n* carbon planes.

Pure graphite is a semimetal with a very low density of states near the Fermi energy (4−5 orders of magnitude less than in a metal), due to small overlap of the π bands.[3,4] Intercalation of electropositive (donor) species results in a transfer of electrons to the C layers, which increases the density of charge carriers in the conduction band (π^*) and determines a rise of the conductivity *parallel* to the C layers. The amount of charge transfer from valence 4s states of K to the graphite host is almost complete in KC_8[2,5] and KC_{24}.[6] Changes in the conductivity perpendicular to the C layers are determined by varying the interlayer distance, which affects the amount of overlap of the C wave functions perpendicular to the graphite sheets. These changes may be brought about by transitions between different stages of intercalation.

Ternary potassium-ammonia GICs of composition $KC_{24}(NH_3)_x$ were first prepared in 1954, and they have been the subject of numerous experimental studies[6−11] which have provided a considerable amount of information on the general structure of the intercalant layers and on the effect of interlayer separation. Important structural changes are brought about by varying the composition of the K-NH_3 layers. In particular, a transition from stage-II ($I_c = 8.74$ Å) to stage-I ($I_c = 6.65$ Å) has been characterized, which is induced by increasing the number of ammonia molecules in the range $0.05 < x < 1.0$, and is associated with an increase of 2 orders of magnitude of the resistance perpendicular to the carbon planes. No satisfactory model has been formulated so far to explain this phenomenon.

Proton nuclear magnetic resonance (NMR) and X-ray studies carried out on $KC_{24}(NH_3)_{4.33}$[7,8,12] have shown that potassium ions and ammonia molecules form only monolayers in the graphite galleries, with both potassium and ammonia rapidly diffusing at room temperature. Ammonia molecules are also rotating rapidly on the NMR time scale around their C_3-axis which is tilted with respect to the *c*-axis and precessing around it. The tilt angle is itself fluctuating dynamically around an average value of 77° with regard to the *c*-axis. Although rapid hopping diffusion on the lattice sites cannot be ruled out by the NMR measurements, the liquidlike behavior appears to be a key feature of the intercalant layers and qualifies the K-NH_3 GICs as the two-dimensional structural analogues of bulk potassium-ammonia solutions.[8]

Despite the large amount of experimental data, the available picture of intercalant species is far from complete. In particular,

* Author to whom correspondence should be addressed.

10.1021/jp012466p CCC: $22.00
Published on Web 01/18/2002

detailed information on the intercalant structure and short time scale dynamics is still lacking. Recent time-of-flight neutron diffraction studies[13] allowed the out-of-plane structure of the compound $KC_{24}(NH_3)_{4.3}$ to be resolved, leading to the surprising result that the interlayer potassium ions are located in two peaks adjacent to the graphite sheets, rather than at the mid-plane. The tilt of the C_3-axis of the NH_3 molecules enables them to orient the positive ends of their dipoles directly away from the potassium ions. The nitrogen atoms are located exactly in the mid-plane, and the occurrence of three distinct peaks in the proton neutron scattering density profiles supports hindered tunneling rotation about the C_3-axis, observed in cesium intercalates at low temperature.[14]

Gaining more detailed knowledge of the structure and dynamic properties of the intercalant is an important task not only in itself. Indeed, much of the current interest in the ternary metal-ammonia GICs arises from their peculiar electronic and optical properties and in the possibility of tuning them by changing the composition of the intercalant. Measurements performed in the composition range $0 < x < 4.38$ [15] have shown that at high NH_3 loading ($x > 4$), resistance *parallel* to the carbon layers first increases and then shows a shallow but notable decrease. Optical studies[16] have identified features in the reflectance spectra and in the complex dielectric function for $x \simeq 4$ that can be explained by assuming the presence of localized electronic states in the intercalant. In particular, a sharp band in the frequency-dependent complex dielectric function located at $\hbar\omega = 1.85$ eV with fwhm of 0.4 eV, which appears to be characteristic of GICs of this composition, strongly resembles a corresponding feature at $\hbar\omega = 0.8$ eV with similar fwhm described in metal-ammonia solutions, which has been shown to arise theoretically[17] from transitions between 1s and 2p hydrogenic states of an electron trapped in a spherical cavity of NH_3 molecules of ~6 Å diameter. In addition, a Lorentzian curve fitting of the line shape of the GIC adsorption band has shown an increase in the oscillator strength up to $x = 4.11$, followed by a sudden drop at $x = 4.38$.[16] This is seen as evidence for a transition from strongly localized states, arising from charge density back-transfer from the carbon layers to "solvation" sites in the intercalant[18] (or from a partial sharing of electron density between the carbon layers and the potassium ion[13,15]), up to a threshold after which delocalization parallel to the carbon planes occurs within the intercalant and determines the observed decrease in resistance and the drop in the 1.85 eV band oscillator strength. The mechanism of this two-dimensional metal-nonmetal transition is thus closely related to the corresponding three-dimensional transition in metal-ammonia solutions, of which the ternary metal-ammonia GICs are thus the two-dimensional electrical analogue. Understanding the interrelation between structure and electronic properties is of great importance, as electron transfer between carbon layers and the intercalant are largely determined by the local environment of the site which electronic charge is being transferred to. Conversely, the presence of more or less localized states may play a role in shaping the structure of the intercalant and in determining its dynamic properties.

In this paper we present results concerning the static properties of a series of stage-I binary (KC_8 and KC_{24}) and ternary ($KC_{24}(NH_3)_x$, $x = 1, 2, 3, 4, 4.5, 5$) potassium and potassium-ammonia GICs. For each species, geometry optimizations were performed (allowing full ionic relaxation) based on DFT[19] total energy and interionic force calculations. In addition, we performed FPMD simulations at different temperatures (373−573 K) on a selected number of systems, namely KC_8, $KC_{24}(NH_3)_4$, and $KC_{24}(NH_3)_5$. In the case of KC_{24} (which is experimentally known to be a stage-II compound), we analyzed the effect of varying the interlayer separation on the structure and energetics of the system and we performed a full unit cell optimization.

II. Structures and Details of Calculations

The systems examined in this work can be formally derived from the hexagonal crystal of pristine graphite in its Bernal structure (Figure 1). This is characterized by planes of carbon atoms (with a nearest neighbor distance of 1.42 Å) stacked above each other at a vertical distance of 3.40 Å. Successive planes are displaced laterally, so that a carbon atom belonging to a plane labeled B is located exactly above the center of a hexagon of carbon atoms of an A plane. The crystal belongs to the space group P 6_3/m m c (194) with primitive unit cell vectors $a = b = 2.46$ Å, $c = 6.80$ Å, $\alpha = \beta = 90°$, and $\gamma = 120°$,[20] and a vertical repeat distance $I_c = c$. The representation of the intercalated species in the simulations has been obtained by replacing each B layer with a layer of potassium or potassium and ammonia. Each periodically repeated unit cell of a system of composition $KC_y(NH_3)_x$ thus contains one layer of y carbon atoms and one layer of potassium or potassium-ammonia intercalate. We are thus not able to address the mechanism of staging in this work. For the same reason, information on correlation effects in the motion of ions belonging to different layers is not accessible, and the out-of-plane dynamics of the K atoms in different layers takes place with all the atoms moving in phase. The a and b vectors of the unit cell were determined by considering supercells obtained by duplicating in the ab-plane one graphite primitive cell and commensurate with the unit formula of the compound.[1] Before ionic relaxation, the K atoms were placed above the center of carbon rings and approximately in the plane between the two carbon layers. The vertical repeat distance I_c for C_8K was set equal to the experimental value[21] (5.35 Å), while for the ammoniated species the value $I_c = 6.65$ Å was chosen, corresponding to the repeat distance in the stage-I compound $KC_{24}(NH_3)_{4.3}$.[13] This same value was adopted for KC_{24}, though in this case a repeat distance was obtained of 6.89 Å from unit cell optimization. Each system consists of one periodic supercell of 24 C atoms and 1 K atom (apart from $KC_{24}(NH_3)_{4.5}$ which contains 48 C atoms and 2 K atoms) plus the relevant number of NH_3 molecules required to complete the formula unit.

DFT-FPMD simulations[22] were performed by integrating classical equations of motion for the ionic system using first-principle interionic forces which were computed, in the adiabatic approximation, by self-consistently minimizing the total energy at each time step of ionic relaxation.[23,24] A Pulay density mixing conjugate gradient solver was used yielding a convergence in the total energy of 0.00008 eV/atom. The Kohn−Sham eigenvalues were extrapolated at each step of ionic dynamics using a Verlet algorithm. Integrals in the irreducible edge of the Brillouin zone were estimated by quadrature[25] over 1 to 4 **k** points, and the Kohn-Sham eigenvalues were expanded in plane-waves at each **k** point up to an energy cutoff of 200 eV. Vanderbilt ultrasoft pseudopotentials[26] with *s* and *p* nonlocal projectors (with the exception of H, for which only *s* nonlocality was included) were used to model the electron ion interactions. For K, 3s and 3p *semivalence* states were explicitly considered. The exchange-correlation contribution to the total energy was computed within the generalized gradient corrected local density approximation.[27] The temperature during the simulations was controlled via a Nosé thermostat with thermostat capacity 0.00089. The time step for the ionic propagation was 0.5 fs.

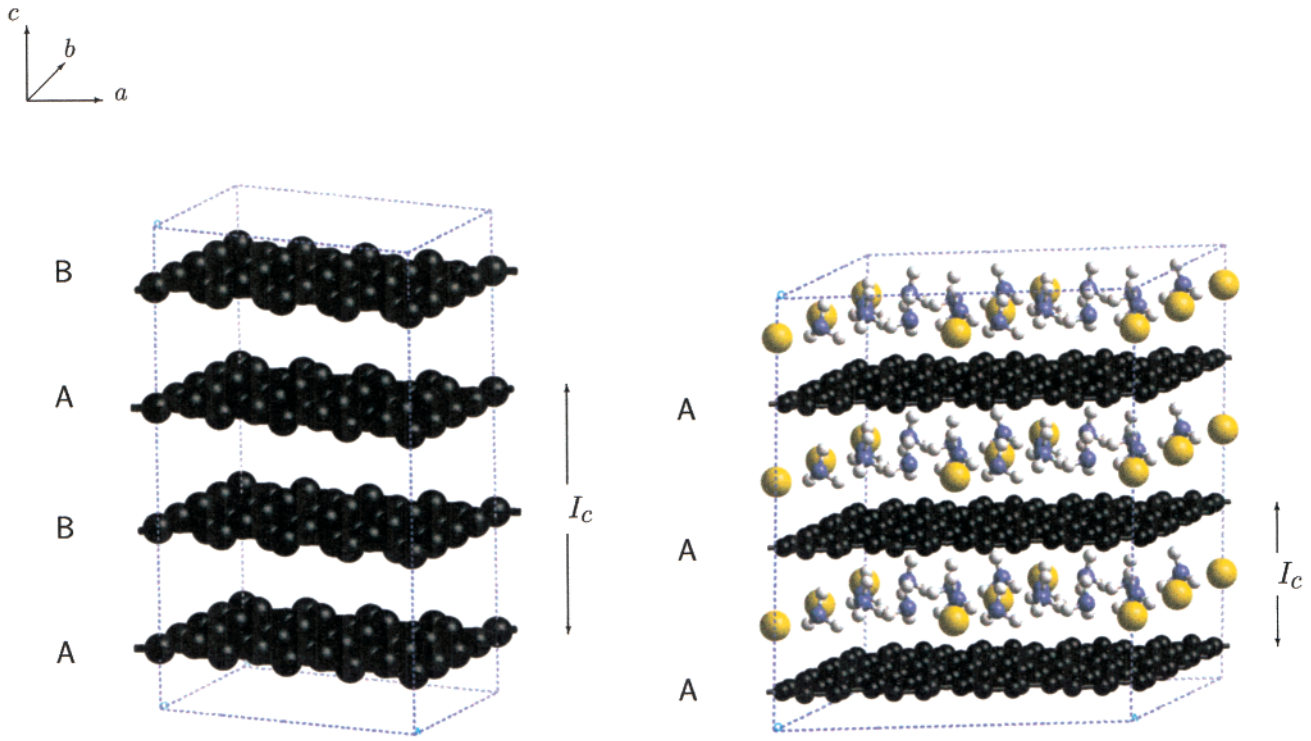

Figure 1. Structure of hexagonal graphite (left) and of a typical stage-I ternary potassium-ammonia GIC ($KC_{24}(NH_3)_4$). Dashed lines represent supercells of 3 × 3 × 2 (graphite) and 2 × 2 × 2 (GIC) unit cells.

The simulation were started from the optimized geometries with random initial ionic velocities, after which the thermostat was applied. Higher temperature dynamics were typically restarted from a set of NVT ionic positions and velocities of a lower temperature simulation. Since each periodically repeated unit cell in our systems contains only one carbon layer, and the interlayer distance does not change during the course of a dynamic simulation, we decided to keep the position of the carbon layers fixed during the course of the dynamics. This has the advantage of requiring a shorter time for thermal equilibration during the initial stages of a simulation. Typical equilibration times were allowed of 1.0−1.5 ps.

Geometry optimizations were performed using the Broyden-Fletcher-Goldfarb-Shanno (BFGS) algorithm, as implemented in CASTEP 4.2, allowing full ionic relaxation. Three criteria were required to be simultaneously satisfied at the optimized geometry, namely RMS of the forces acting on the ions lower than 0.05 eV/Å, RMS displacement of the ions lower than 0.001 Å, and RMS of the total energy lower than 0.0002 eV/atom.

All the systems studied in this work (with the exception of $KC_{24}(NH_3)_{4.5}$, which is treated, in practice, as $K_2C_{24}(NH_3)_9$) contain an odd number of electrons per unit cell. For this reason, spin polarization ought to be taken into account explicitly, leading to twice as many Kohn-Sham states at each **k** point as in the corresponding nonspin polarized systems. It is nevertheless possible to consider fictitious systems in which the last electronic band is automatically filled in, thus avoiding a doubling in the number of states, which obviously result in tremendous computer memory and time savings. We thus performed the majority of the calculations presented in this work neglecting the effects of spin polarization. In a few cases (which will be described in due course), we compared results obtained with and without spin polarization and we typically found that including spin polarization does modify the nonspin polarized results, but only to a limited amount. In particular, no *substantial* changes are observed in the optimized geometries, though differences in the total energies at fixed ionic configurations may be within 0.07 eV. Details of the calculations are summarized in Table 1.

TABLE 1: Cell Parameters, Number of Electronic States and of k Points Included in the Brillouin Zone Sampling, Temperature, and Simulation Times for FPMD

system	*a*, *c* (Å)	electronic states per unit cell[a]	**k** points in BZS	FPMD simulations
KC_8	4.92, 5.54	21 (41)	4	373 K (4.0 ps) 573 K (2.0 ps)
KC_{24}	8.52, 6.65	53	4	373 K (2.40 ps) 573 K (4.00 ps)
	8.52, 5.83	53	4	
	8.52, 6.89	53	4	
	8.52, 8.74	53	2	
$KC_{24}(NH_3)$	8.52, 6.65	57	4	
$KC_{24}(NH_3)_2$	8.52, 6.65	61	4	
$KC_{24}(NH_3)_3$	8.52, 6.65	65	4	
$KC_{24}(NH_3)_4$	8.52, 6.65	69 (137)	4	373 K (2.7 ps)
			4	573 K (2.9 ps)
$KC_{24}(NH_3)_5$	8.52, 6.65	74	4	573 K (2.1 ps)
$K_2C_{48}(NH_3)_9 \equiv [KC_{24}(NH_3)_{4.5}]_2$	$a = 17.04$ $b = 8.52$ $c = 6.65$	141	1	

[a] Values in curves refer to spin-polarized calculations.

III. Structure and Dynamics in KC_8 and KC_{24}

In C_8K and $C_{24}K$, the alkali metal atom is located exactly above the center of a graphite hexagon. This adsorption site ("hollow") appears to be the most favorable (with respect to "bridge"—above a C−C bond—, and "on-top"—above a C

TABLE 2: Optimized Geometric Parameters for Potassium and Potassium Ammonia GICs[a]

system	K−C layer (Å)	K−N (Å)	NK̂N (deg)	N−H (Å)	HN̂H (deg)
KC_8	2.770				
KC_{24} $I_c = 6.65$	2.800				
$I_c = 5.83$	2.901				
$I_c = 6.89$	2.998				
$I_c = 8.74$	2.684				
$KC_{24}(NH_3)$	3.281	2.775			
$KC_{24}(NH_3)_2$	3.211	4.576, 5.861	172.76		
$KC_{24}(NH_3)_3$	3.144	2.728, 2.732, 4.761	135.96 (*t*), 65.53, 72.78 (*c*)		
$KC_{24}(NH_3)_4$	3.186	2.828	167.67 (*t*), 89.43 (*c*)	1.017	109.36
$KC_{24}(NH_3)_4$ (sp)	3.291	2.856	168.70 (*t*), 89.73 (*c*)	1.017	108.80
$KC_{24}(NH_3)_{4.5}$	3.344	2.830, 4.844	150.71, 176.53 (*t*), 73.41, 77.30, 105.15, 104.78 (*c*)	1.016	109.93
$KC_{24}(NH_3)_5$	3.240	2.809, 3.549	147.93, 166.41 (*t*), 69.97, 77.98, 88.51, 123.56	1.018	109.32
$K(NH_3)_4^+$ (gas phase)		2.922	158.12 (*t*), 88.25 (*c*)	1.018	107.39

[a] In the first column, (sp) indicates spin-polarized calculations. In the third column, for $x \geq 4$, K−N distances have been averaged over the 4 ammonia molecules, and the additional value corresponds to the K−N distance for the fifth molecule. In the fourth column, (*t*) and (*c*) indicate trans and cis ammonia molecules with respect to K. NH distances and HN̂H angles are averaged over *all* the ammonia molecules in the unit cell.

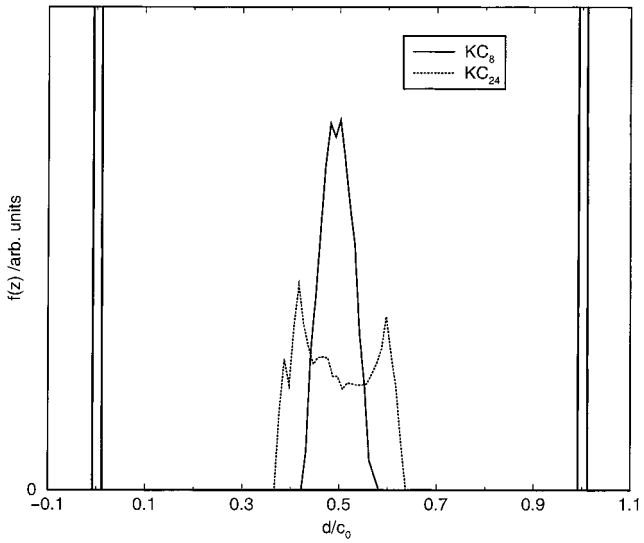

Figure 2. K−C layer distance distribution functions for KC_8 and KC_{24} during FPMD at 373 K. Vertical lines near the boundaries of the figure represent the carbon planes.

atom− positions) also from DFT (LSDA and GGA) cluster calculations of K adsorption on the graphite surface.[28] In the former species, K is located midway between two C-layers (within 0.01 Å), while in the latter it is much closer to one of them (Table 2). This suggests that the interaction of K with a C-layer in $C_{24}K$ is similar to the adsorption on a graphite surface, perturbed by the presence of the second neighbor layer. Indeed, the distance between K and the nearest C-layer in $C_{24}K$ (2.800 Å) is very close to the one calculated for the adsorption on the graphite surface (2.77−2.82 Å).[29]

The different nature of the K−C interactions in the two compounds is mirrored by the behavior of the alkali metal atom during finite temperature FPMD simulation at 373 K. The distribution of the K−C layer distances in the two species is shown in Figure 2. In both cases, K oscillates in the *z*-direction (perpendicular to the carbon planes). The KC_8 distribution is very sharp and has only one maximum in the mid-plane (though a slight splitting may be discerned at the top). The KC_{24} one has two well distinguished maxima symmetrically located with respect to the mid-plane.

To understand the origin of these different features in the two systems, we computed the magnitude of the force acting on K in the *z*-direction, when the alkali metal atom is displaced perpendicular to the carbon planes with the *x*- and *y*-coordinates fixed at the optimized values. We repeated this calculation on KC_{24} at several values of I_c (5.83, 6.65, 6.89, and 8.74 Å). For KC_8 we performed this analysis with and without spin polarization, to figure out if and to what extent this may modify the amplitude of the forces. Results are shown in Figure 3.

The overall shape of the $F(z)$ curve is largely determined by the distance between the carbon layers and it depends only slightly on the number of K atoms in the unit cell. In particular, the shape in the vicinity of the minimum (see inset in Figure 3) is approximately the same in KC_8 and KC_{24} ($I_c = 5.83$ Å), denoting a strong similarity in the interactions which determine the K position between the two planes. Including spin polarization in KC_8 leaves the overall curve essentially unchanged. Increasing the interlayer spacing in KC_{24} to 6.65 Å (the stage-I interlayer separation) results in a lowering of the forces acting on K when in the mid-plane and the appearance of two symmetric minima above and below it, consistent with our findings that K is not in the mid-plane in the optimized structure and that two maxima appear in the distance distribution for this system.

Further increase of the interlayer spacing to 6.89 Å (our DFT optimized interlayer separation for a stage-I compound of this composition) causes the $F(z)$ curve to become nearly flat in the vicinity of the minimum, with the two symmetric minima almost completely disappearing. However, two rather narrow minima do appear in this system at much shorter distance from the carbon layers (approximately 2.5 Å from the closest carbon layer, though this value may carry a large uncertainty owing to the interpolation procedure). It is interesting to note that these two minima correspond to forces which are only ∼0.02 eV/Å larger than the force in the mid-plane. In fact, we found that, in the optimized geometry, K does reside in one of these minima, rather than in the mid-plane, at a distance of 2.549 Å from the closest carbon layer. Although we did not carry out any finite temperature simulations on this system, we can infer that they would be characterized by a very wide distribution of C−K distances, arising from diffusion of K among the three minima, and, possibly, depending on the temperature, by the presence of three well-defined maxima.

Finally, as I_c is set equal to 8.74 Å the two symmetric minima (at a distance of ∼2.6 Å from the C planes) correspond to forces which are ∼0.06 eV/Å larger than at the central minimum. The very high barriers between the minima (∼0.25 eV/Å) would hinder the diffusion of K between them, confining its oscillations (at least at moderate temperatures) to occur at a well-defined position, either in the mid-plane or closer to the carbon layers.

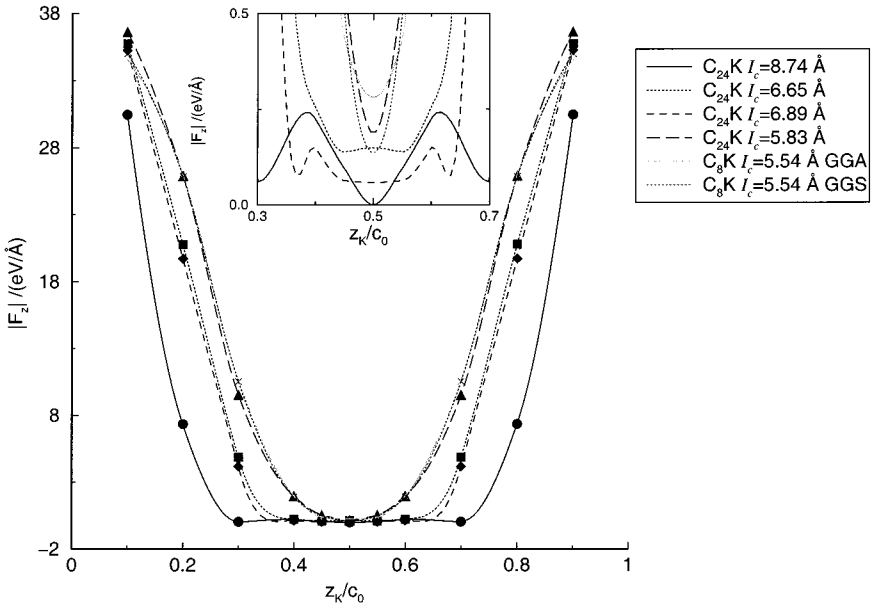

Figure 3. Force acting on K in the direction perpendicular to the carbon planes. Forces have been computed only in correspondence to the points indicated, and for $0.1 \leq z_K/c_0 \leq 0.5$, the $0.5 < z_K/c_0 \leq 0.9$ having been extrapolated assuming $F(z_K/c_0 + 0.5) = F(z_K/c_0 - 0.5)$. Curves have been obtained by interpolation with splines and have been shifted in the inset for clarity. GGA and GGS indicate nonspin polarized and spin polarized calculations, respectively.

We can qualitatively account for these findings by considering the interactions shaping the potential curves during the displacement of K perpendicular to the carbon planes. Assuming the 4*s* electron to be completely transferred to a carbon layer, the equilibrium position of the cation between the negatively charged layers would be determined by (*a*) Coulombic attraction with each of the layers, and (*b*) exchange−repulsion between core states of K and partially filled π^* graphite states. In the absence of the former interaction, the $F(z)$ curve would have one minimum in the mid-plane. Since interactions of type (*b*) are very short-ranged, the shape of the $F(z)$ curve would vary from that of a narrow minimum to a very flat plateau (with $F(z) \simeq 0$), depending on the interlayer separation. In the first case, (*b*) would largely overcome (*a*), and K would find itself confined within a narrow (exponential) potential well in the mid-plane. As I_c is increased and the repulsive potential tends to flatten in the mid-plane region, the attractive contribution (*a*) starts growing in importance, leading to the appearance of minima in the $F(z)$ curve between the mid-plane and each of the carbon planes. This is roughly what is observed in KC_{24} when I_c is increased from from 5.83 to 6.65 Å. The occurrence of a well-defined minimum at the mid-plane in KC_{24} at $I_c = 6.89$ and $I_c = 8.74$ Å cannot be explained by this simple model. We suggest that, in this case, the assumption of a complete transfer of the 4s electron to graphite does not hold when K is confined in the vicinity of the mid-plane, and further work is in progress to examine this suggestion.

The motion of K parallel to the carbon planes can be easily interpreted from the vibrational density of states (VDOS) (Figure 4), computed from the velocity-velocity self-correlation function (resolved into its in-plane and out-of-plane contributions) for the K atom alone. Zero density at $\omega = 0$ cm^{-1} in KC_8 denotes the absence of diffusion of K at 373 K. K is thus vibrating above and below the mid-plane with a main frequency of 67 cm^{-1}. The oscillatory motion in the *xy*-plane is slower (23 cm^{-1}).

The corresponding VDOS plot for KC_{24} ($I_c = 6.65$) is shown in Figure 5. The broad peak at zero frequencies at both low (373 K) and high (573 K) temperature in the in-plane component denotes diffusion of K in the *xy*-plane. Two dominant peaks

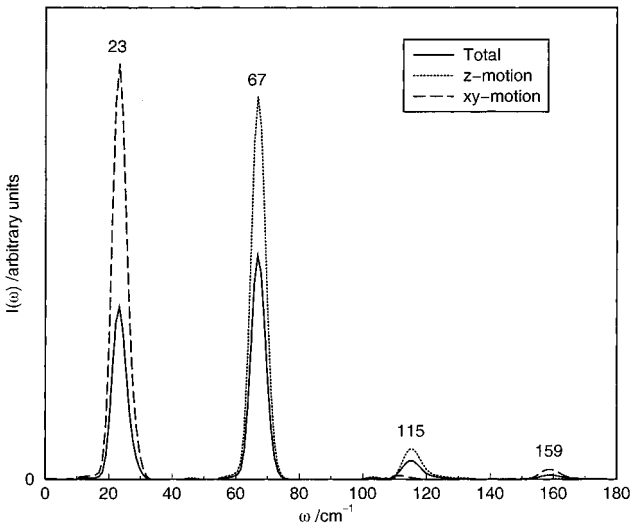

Figure 4. VDOS for KC_8 at 373 K.

appear in the *z*-component, at 23 and 31 cm^{-1} (the former only at higher temperature). In view of the findings described in the previous paragraphs, we argue that the presence of fast vertical fluctuations at lower temperature corresponds to K oscillating preferentially in one of the potential minima, while the onset of slower oscillations at higher temperature can be explained by more frequent diffusion between the two minima which allows K to span a larger portion of the potential well along *z*.

A shorter FPMD simulation was performed on KC_8 at 573 K, for which the VDOS is shown in Figure 6. At this temperature, diffusion of K in the *xy*-plane sets in. Also, the frequency of vibration perpendicular to the carbon planes increases by ∼10 cm^{-1}. This shift is connected to a change in the shape of the K−C layer distance distribution with respect to the lower temperature simulation (Figure 7). In this case, the appearance of two sharp maxima cannot by attributed to changes in the perpendicular force profile, but rather to K experiencing in turn potential wells of different width during its diffusive motion.

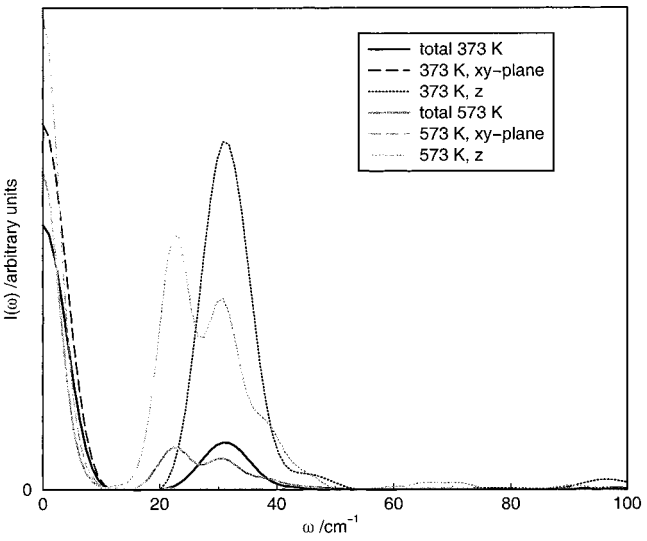

Figure 5. VDOS for KC_{24} at 373 and 573 K.

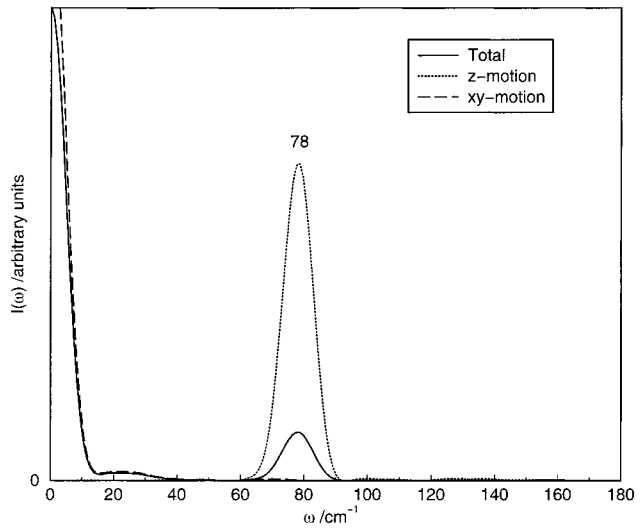

Figure 6. VDOS for KC_8 at 573 K.

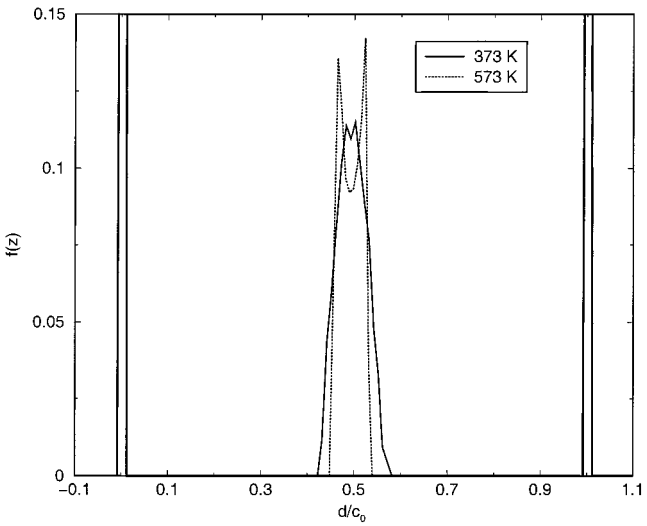

Figure 7. K−C layer distance distribution in KC_8 during FPMD at 373 and 573 K.

The results for the in-plane plane motion for KC_8 and KC_{24} are summarized in pictorial form in Figure 8. The occurrence of in-plane diffusion in KC_{24} is consistent the high mobility of K adsorbed on a graphite surface which has been reported for $T > 90$ K.[30−32] We also find that different diffusion paths are possible, depending on the temperature, and (possibly) on the initial conditions of the trajectory. In KC_{24}, at low temperature, diffusion between hollow sites above different carbon rings appears to take place by almost uni-dimensional translation parallel to the *a*-axis, while at higher temperature an on-top → on-top diffusion sets in. Preferential diffusion along *x* implies that the hopping between different hollow sites takes place by crossing bridge sites only (*i.e.*, moving perpendicular to C−C bonds). Quantitative estimates of the diffusion potential energy barrier for the hollow-bridge and hollow-top path have been determined for K adsorbed on a graphite surface.[28] Although the energy barrier appears to be comparable in the two cases, a top site is characterized by a minimum on the potential energy surface (only ∼0.5 eV less stable than a hollow site), while a bridge site corresponds to the center of a wide and flat maximum at an energy of 2.0 eV higher than that of the hollow site. This would suggest that the hollow-top diffusion (e.g., diffusion along *y* only) is more favorable. However, pure diffusion along *y* would imply a sequence of elementary steps hollow → top → bridge → hollow, while *x*-diffusion would only require hollow → bridge → hollow steps. This would make the *x*-direction a preferential channel for diffusion. Our findings do indeed support this argument, though they also point to the possibility for the system to explore alternative diffusion paths, depending on the temperature and on the starting position of the cation. Also, it should be remarked that the presence of the second graphite layer in the intercalated system would modify the motion of K with respect to a single graphite surface, decreasing the energy of adsorption onto a single graphite plane.

IV. Structure and Dynamics in the K/NH_3 Intercalates

1. $KC_{24}(NH_3)_x$, $x = 1, 2, 3$. The inclusion of 1 NH_3 molecule determines, in the optimized geometry, a displacement of the alkali metal atom away from the hollow site toward an on-top one (Figure 9). Indeed, K turns out be almost exactly in the mid-plane (only 0.044 Å from it), and very close to an on-top site. The K−N distance is particularly short (2.775 Å, to be compared with the experimental K−N distance in $KC_{24}(NH_3)_{4.3}$,[13] 2.88 Å), and the C_3-axis of the NH_3 molecule is oriented toward K. Thus, NH_3 is pointing its dipole moment directly away from K. The N atom is very close to the mid-plane (∼0.1 Å *above* it, with respect to K which is below), and the tilt angle of K−N with respect to the graphite planes is around 5°.

The situation is quite different when two NH_3 molecules are included in the unit cell. K returns to occupy a hollow site, at 0.114 Å from the mid-plane. The N atoms are also in the mid-plane, but their distance from K (4.576 and 5.861 Å) and the orientation of the C_3-axis in each NH_3 molecule (unrelated to the position of K) suggests that no strong charge−dipole interactions between K and NH_3 are present in this system.

In the $x = 3$ system only two NH_3 molecules (at 2.728 and 2.732 Å) appear to be coordinated to K, though also the C_3-axis of the third molecule (at 4.761 Å) is approximately oriented toward K. The alkali metal atom is now slightly closer to a C layer than it was in the previous system (the distance from the mid-plane now being of 0.181 Å), and it is located midway between a hollow and an on-top site, while the nitrogen atoms are again almost exactly in the mid-plane. The N− K̂−N angle (where N belongs to one of the closest NH_3 molecules) is 135.9°, which suggests that the linear $H_3N\cdots K\cdots NH_3$ coordination is not a particularly favorable one in this situation.

2. $KC_{24}(NH_3)_x$, $x = 4, 4.5, 5$. In the optimized geometry, $KC_{24}(NH_3)_4$ is characterized by K occupying a hollow site at a

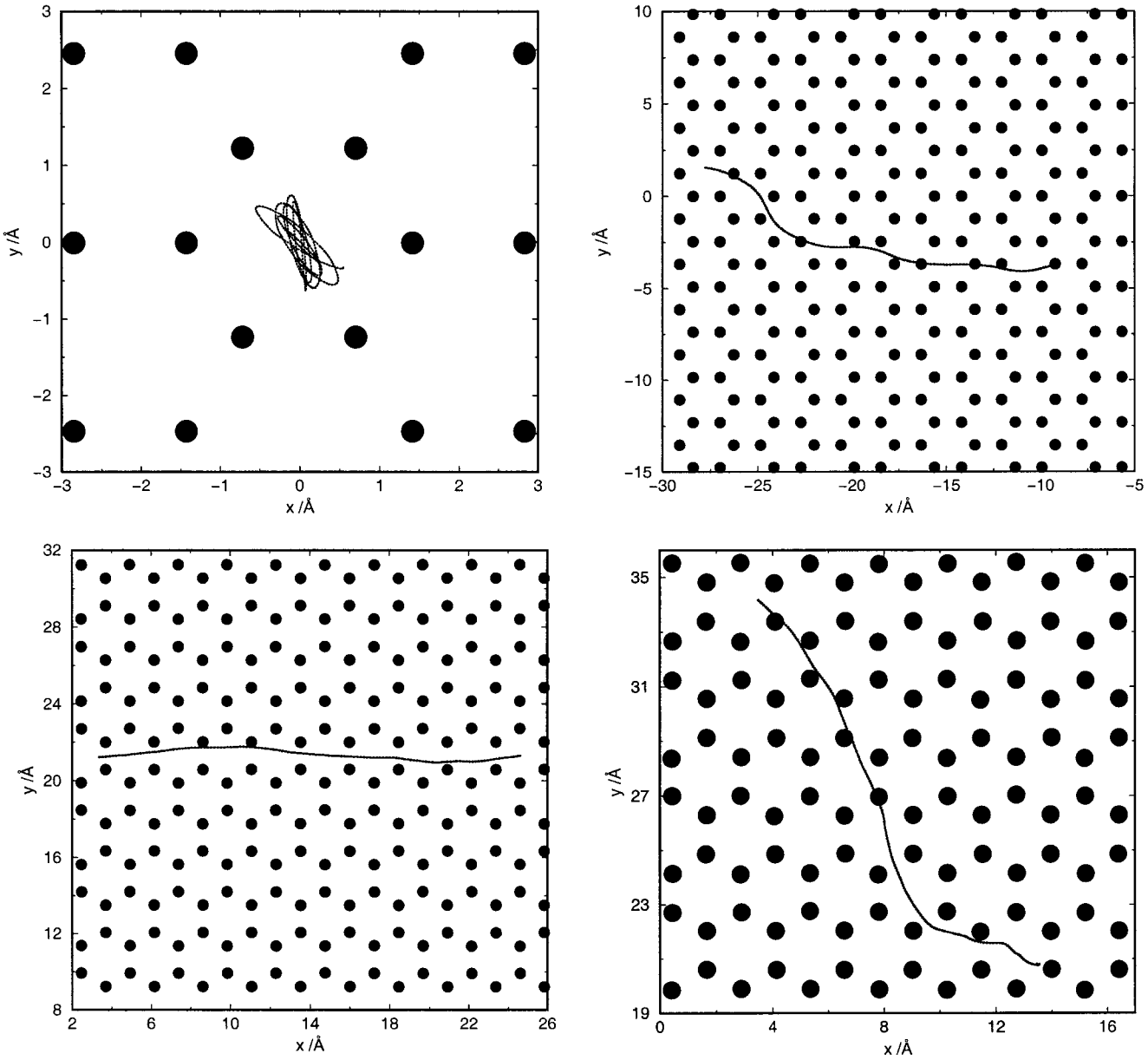

Figure 8. K trajectories in KC_8 at 373 K (upper left) and 573 K (upper right) and in KC_{24} at 373 K (lower left) and 573 K (lower right), as seen perpendicular to the carbon planes. Dots represent C atoms.

vertical distance of ∼3.2 Å, and by rather short K−N distances (∼2.8 Å) for all the four NH_3 molecules which are pointing their C_3-axis directly toward K. The intercalated $K(NH_3)_4^+$ clusters are nonplanar, with the four NH_3 molecules pointing their dipoles away from K^+. The angle between the N−K bond and the plane containing the four N atoms is of approximately 5.5° (Table 2). Including spin polarization changes the calculated parameters only slightly, the notable exception being in the position of K, now much closer to the mid-plane. The K−N tilt angle is reduced to 4.6°.

For comparison, we performed a full optimization on the structure of the free compound $K(NH_3)_4^+$, whose parameters are also shown in Table 2. The geometries of the free and of the intercalate compound are very similar. K−N distances are ∼0.1 Å larger in the gas-phase compound and $\hat{NKN}$ angles are smaller (∼10° for trans and ∼1° for cis NH_3 molecules). The tilt angle of the N−K bond with respect to the plane containing the N atoms is ∼13° in the gas-phase species. $\hat{NKN}$ angles are closer to the experimental value for gas-phase NH_3 (107°,[1]) in the free cluster. Larger $\hat{NKN}$ angles in the intercalated moiety with respect to the gas phase imply a change in the hybridization of N from ∼sp^3 toward sp^2 + p. On one hand, this decreases the dipole moment of NH_3, weakening the charge-dipole contribution to the stabilization of the cluster, while, on the other, it reduces the directional character of the lone-pair, allowing K and NH_3 to get closer together. Since all the NH_3 molecules are pointing their dipole away from K, dipole−dipole interactions are destabilizing. This may possibly be the reason for the deviation from planar geometry of the $K(NH_3)_4^+$ clusters. The larger deviation is observed in the gas-phase cluster, consistent with the expected larger dipole moment of the ammonia molecules.

Including a larger number of NH_3 molecules in the unit cell has two main effects. In the first place, it determines a reduction of the symmetry of the $K(NH_3)_4$ clusters which distort in order to accommodate the additional molecule. At $x = 4.5$, the distortion only affects $\hat{NKN}$ angles, leaving the N−K distance for the 4 NH_3 molecules closest to K essentially unchanged, while at $x = 5$, the N−K distances show fluctuations of up to 0.1 Å with regard to the $x = 4$ case. Second, the K atoms reside,

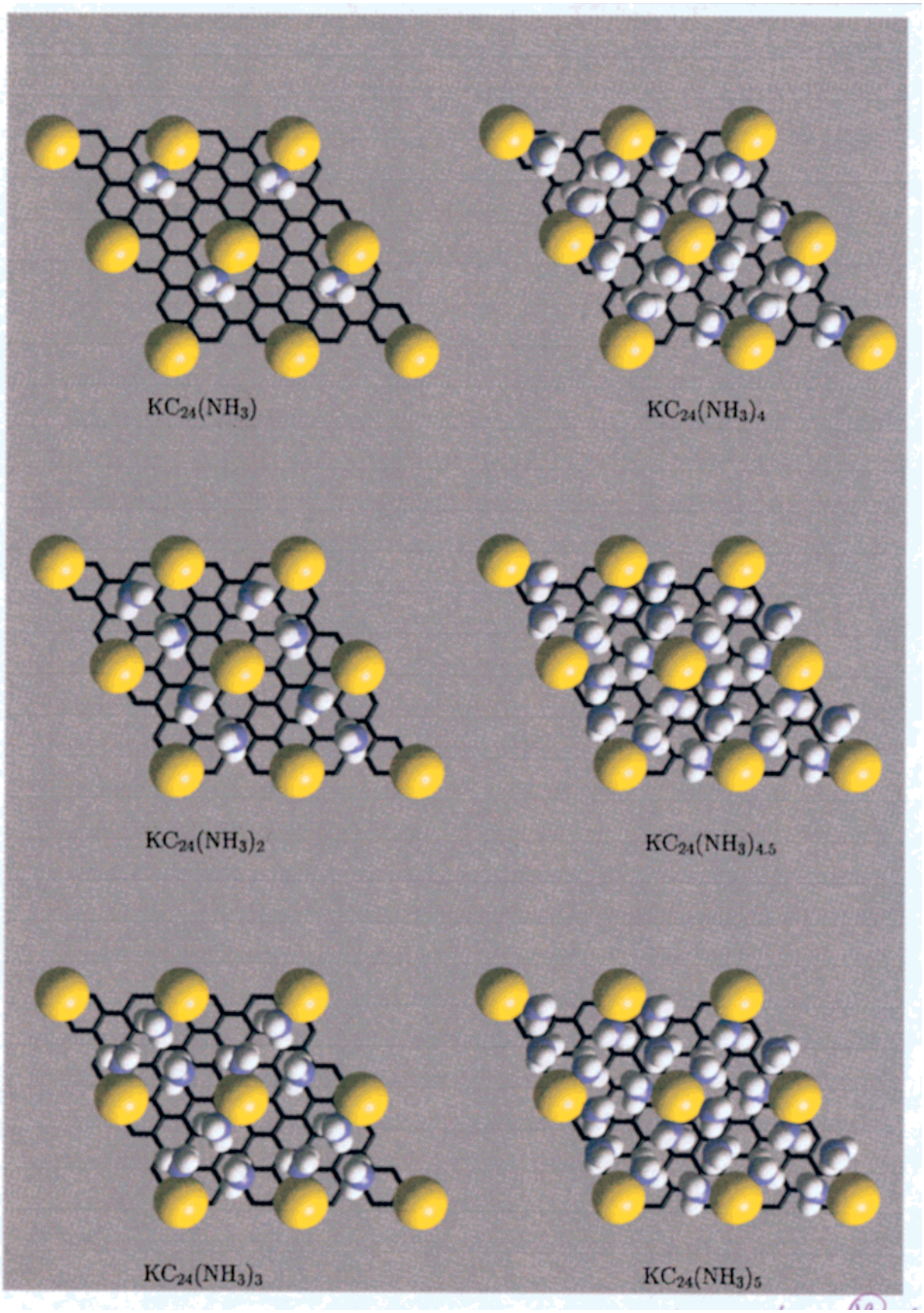

Figure 9. Optimized geometries for ternary potassium-ammonia GICs.

in both cases, exactly in the mid-plane, although slightly displaced from the hollow adsorption site.

Calculations of the force acting on K for displacements perpendicular to the carbon planes were performed for $x = 4$ and $x = 5$. At each position along the path, the NH_3 molecules were allowed to relax to their equilibrium configuration.[33] Results are shown in Figure 10, where the curve for KC_{24} ($I_c = 6.65$ Å) is also displayed for comparison. A drastic change

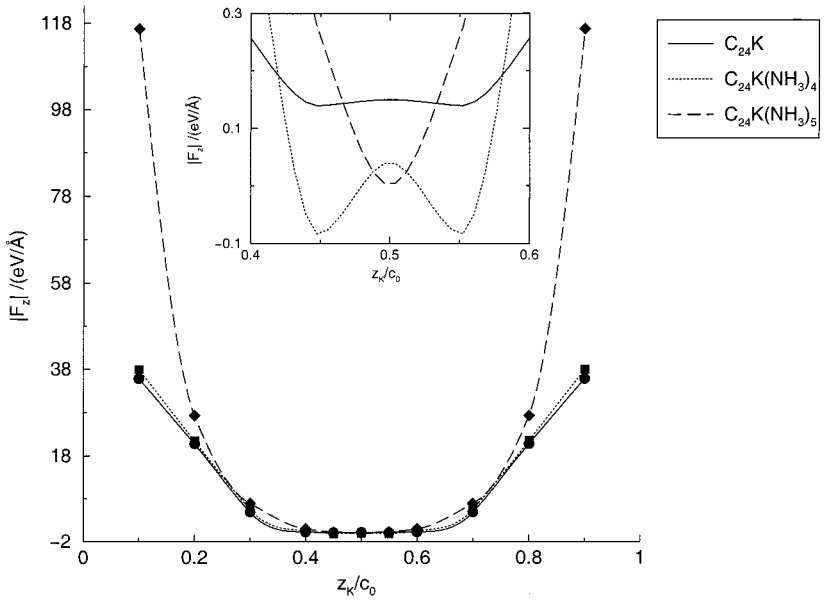

Figure 10. Force acting on K in the direction perpendicular to the carbon planes. Forces have been computed only in correspondence to the points indicated, and for $0.1 \leq z_K/c_0 \leq 0.5$, the $0.5 < z_K/c_0 \leq 0.9$ having been extrapolated assuming $F(z_K/c_0 + 0.5) = F(z_K/c_0 - 0.5)$. Curves have been obtained by interpolation with splines and have been shifted in the inset for clarity.

of character is observed in the $x = 5$ $F(z)$ curve which lacks the double minimum and shows very large forces in the vicinity of the carbon planes. This is not a surprising result, if one takes into account that, in the optimized geometry, K is not in a hollow site, but rather it is displaced toward an on-top one. According to the simple model described in connection with KC_8 and KC_{24}, the potential curve for displacements of K perpendicular to the carbon planes, starting from an on-top site, is dominated, at this interlayer separation, by the exchange−repulsion between K and one of the layers, which would yield a single and rather narrow minimum. This result indicates that the intercalated K is actually experiencing an *effective* interlayer separation which varies according to its adsorption site, and which determines not only a large change in the forces depending on its position (hardly surprising if one takes into account the "roughness" of the graphite layers), but, in many cases, also a variation in the shape of the potential curve.

The distance distribution functions from the carbon layers in $KC_{24}(NH_3)_4$ (at 373 and 573 K) and $KC_{24}(NH_3)_5$ (573 K) are shown in Figure 11. Similar shapes are observed in both systems for each species (K, N, and H). In particular, the K distribution shows two maxima at ±0.46 Å from the mid-plane, while N has one single sharp peak in the mid-plane. The H distance distribution has two main peaks at ±0.62 Å from the mid-plane, though secondary maxima start to appear (at both high and low temperature) closer to the mid-plane in $KC_{24}(NH_3)_4$. The motion of K is, in both cases, very similar to that observed in KC_{24}: the alkali metal atom is diffusing in the *xy*-plane and oscillating perpendicular to the carbon planes. However, diffusion is much more hindered in the ammoniated species, and phases characterized by oscillatory motion in the vicinity of a hollow site may appear, constraining the *xy* motion of K within the limit of a single C_6 ring (Figure 12). Also, the *xy*-plane mobility of K in $KC_{24}(NH_3)_5$ appears to be slightly larger (especially during the diffusive motion) than in $KC_{24}(NH_3)_4$ and the oscillations perpendicular to the carbon planes not as wide. The origin of the mechanism hindering free diffusion of K may reside in a transfer of translational kinetic energy to internal modes of the $K(NH_3)_x^+$ clusters, which has the effect of cooling the motion of K, or in direct interactions between the carbon layers and the ammonia molecules.

The frequencies of the perpendicular motion are 24 and 29 cm^{-1} in $KC_{24}(NH_3)_4$ and $KC_{24}(NH_3)_5$, respectively, only slightly higher than in the unammoniated species (23 cm^{-1}) (Figure 5). This suggests that the vertical oscillations of the cation are largely determined by the interlayer spacing. Since our simulation includes only one carbon layer per unit cell, and the interlayer separation is kept fixed during FPMD simulations, the effects of the vertical relaxation of the layers are fully neglected. Nevertheless, our results remain indicative of the fact that the presence of two maxima in the K distribution function (experimentally observed[13]) are associated with vertical motion of the cation, and, typically, not with K oscillating closer to one carbon layer. This finding has important implications, as short K−C distances may determine a charge back-transfer from the carbon layer to the empty 4s state of the cation,[13,15] thus making a lower amount of electronic charge available for back-transfer from the carbon layers to the solvation sites[18] in the intercalant. We argue that the larger observed mobility of K in $KC_{24}(NH_3)_5$ with respect to $KC_{24}(NH_3)_4$ (induced by the presence of the additional noncoordinating NH_3 molecule) and, above all, the shorter amplitude of the oscillatory motion perpendicular to the carbon planes may prevent K from being too strongly associated with one carbon layer, hindering the back-transfer of charge to the cation and increasing the total electronic charge stored in the [carbon layer + intercalant solvation site] system. This is consistent with the accepted model proposed for the 2D metal−nonmetal transition in potassium-ammonia GICs (taking place between $x = 4$ and $x = 5$),[18] which is explained by electronic delocalization induced by the overlap of the wave functions of electrons initially localized in solvation sites within the intercalant. The balance of the charge redistribution from the carbon layers to either cation states or intercalant solvation sites may thus be crucial in determining whether 2D electron delocalization sets in.

Finally, we examine the internal motion of the $K(NH_3)_x^+$ clusters. A first peak in the K−N pair distribution function (PDF) (Figure 13) is located at ∼2.85 and ∼2.83 Å in KC_{24}-

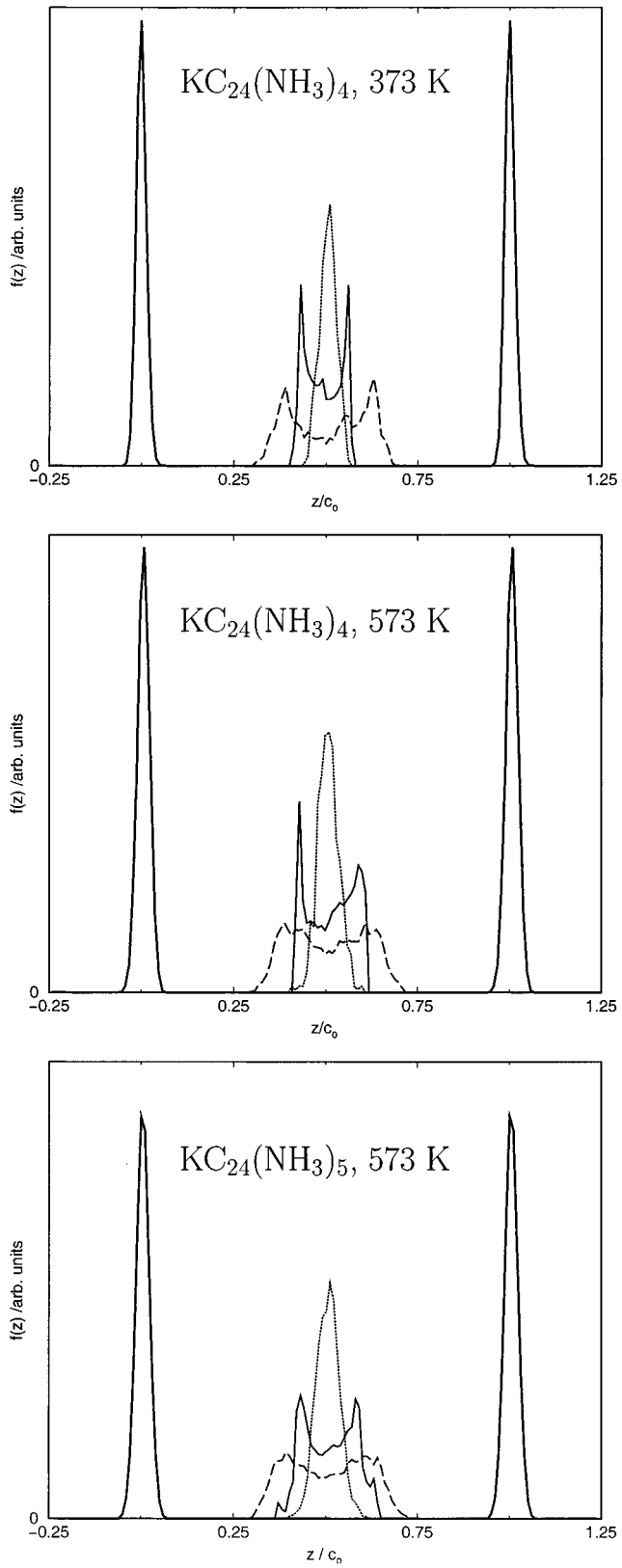

Figure 11. K (solid line), N (dotted), and H (dashed) distance distribution functions from the C layers during FPMDs. Thick solid lines represent the C planes.

$(NH_3)_4$ and $KC_{24}(NH_3)_5$, respectively (to be compared with the experimental K−N distance in $KC_{24}(NH_3)_{4.33}$ of 2.88 Å[13]), and suggests that the ammonia molecules are approximately symmetrically arranged around K in both systems. The peak splits into two main maxima at 2.76−2.91 and 2.79−2.91 Å,

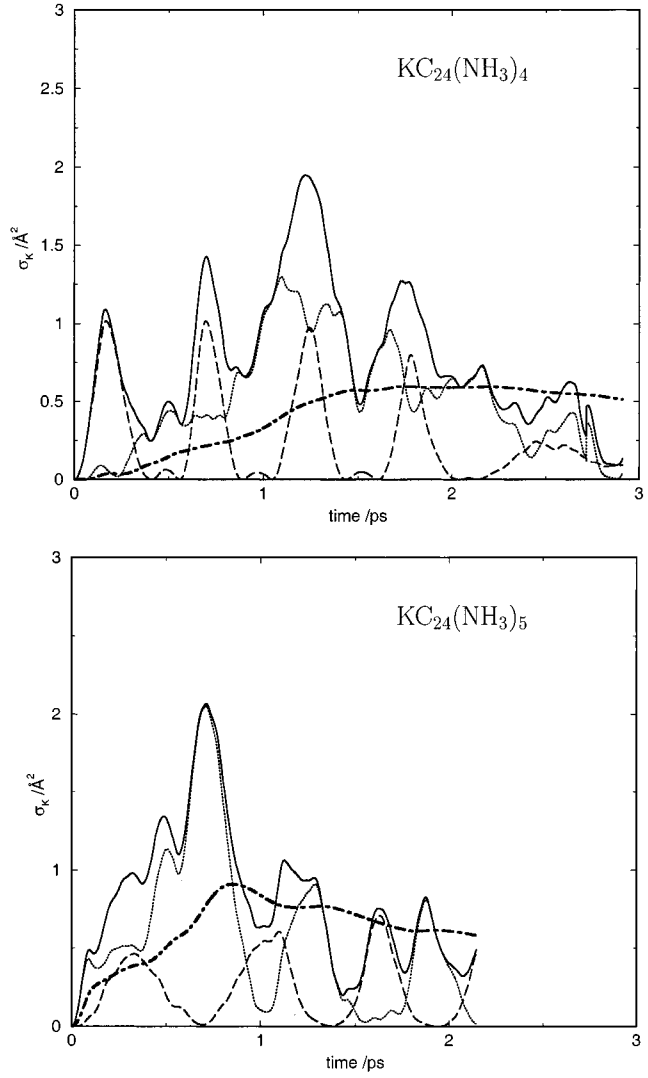

Figure 12. Squared displacements for $KC_{24}(NH_3)_4$ and $KC_{24}(NH_3)_5$ at 573 K, resolved into *xy*-plane and *z*-components. Thick dot−dashed lines represent $\int_0^t dt'\ \sigma_K/t'$.

respectively, possibly indicating a slight asymmetry in the $K(NH_3)_x^+$ complexes. During FPMD, the K−N distances may vary within a range of 2.00 ($KC_{24}(NH_3)_4$, 373 K) to 2.14 Å ($KC_{24}(NH_3)_5$, 573 K). K−H PDFs are less structured and more liquid-like, due to very fast motion of the H atoms. In $KC_{24}(NH_3)_4$, a first broad band appears at 3.23 (373 K) and 3.20 Å (573 K), in both cases characterized by a slight split at the top. In $KC_{24}(NH_3)_5$ the first band is again at 3.23 Å but no splitting is observed. K−H distances vary in ranges of 2.0−2.4 Å in $KC_{24}(NH_3)_4$, and 2.5 Å in $KC_{24}(NH_3)_5$.

From the first peak in the N−K PDFs and the C-layer distance distribution functions we can estimate the average tilt of the K−N bonds with respect to the *ab*-plane, which is 8.7° in $KC_{24}(NH_3)_4$ (373 K), 10.7° in $KC_{24}(NH_3)_4$ (573 K), and 10.2° in $KC_{24}(NH_3)_5$ (573 K). The tilt angle of the NH_3 molecules with respect to the *ab*-plane[34] is ∼11° in $KC_{24}(NH_3)_4$ (373 K), ∼13° in $KC_{24}(NH_3)_4$ (573 K), and ∼10° in $KC_{24}(NH_3)_4$ (573 K). Although these values may carry large uncertainties (which we estimate to be of at most 5°), we conclude that the C_3-axis of the NH_3 molecules is roughly collinear with the K−N bond, so that these are pointing their dipoles directly away from K, in qualitative agreement with the experimental results for $KC_{24}(NH_3)_{4.33}$. Our C_3 tilt angles remain slightly smaller than the experimental value (13°) for this compound, though this may

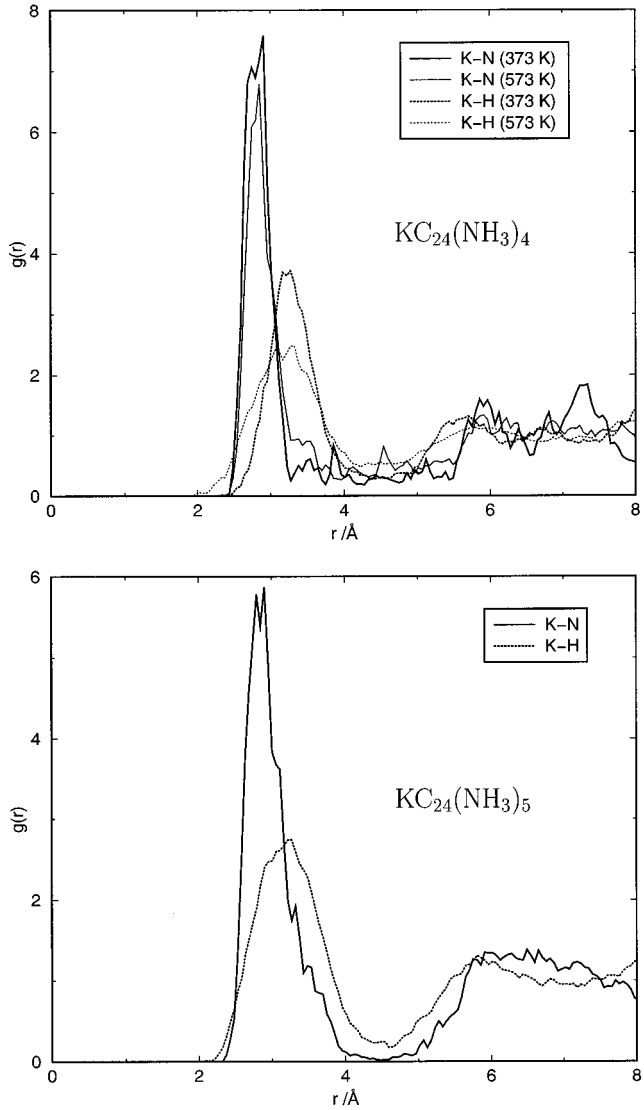

Figure 13. K−N and K−H PDFs for $KC_{24}(NH_3)_4$ (373 and 573 K) and $KC_{24}(NH_3)_5$ (573 K).

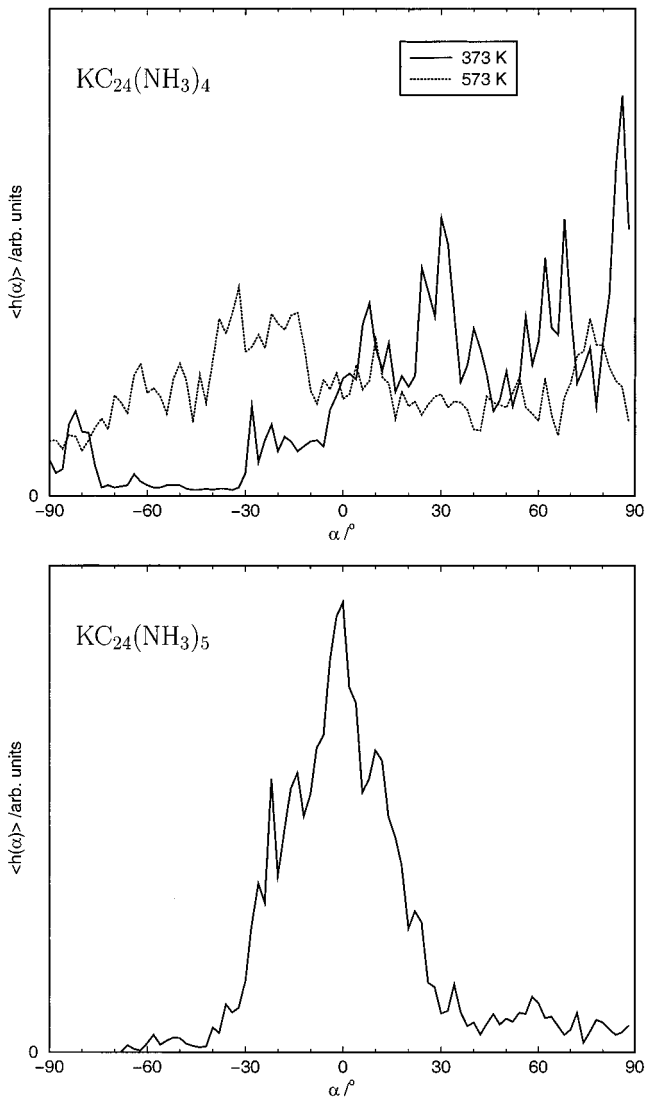

Figure 14. Rotational correlation function distribution, averaged over all the NH_3 molecules in $KC_{24}(NH_3)_4$ (373 and 573 K) and $KC_{24}(NH_3)_5$ (573 K).

be due to neglect of the carbon plane vertical relaxation or to the too short overall simulation times.

To monitor the rotational motion of the NH_3 molecules, we compute the following correlation function:

$$c_i(t) = \frac{\pi}{2} \frac{[\mathbf{R}_H(0) - \mathbf{R}_{C_H}(0)]\cdot[\mathbf{R}_H(t) - \mathbf{R}_{C_H}(t)]}{[\mathbf{R}_H(0) - \mathbf{R}_{C_H}(0)]^2} \qquad (1)$$

where $\mathbf{R}_H(t)$ is the position of one H atom belonging to the NH_3 molecule i and $R_{C_H}(t) = 1/3 \sum_{i=13} \mathbf{r}_j$ is the position of the center of the three hydrogens j belonging to molecule i. We show in Figure 14 the corresponding averaged distribution function

$$\langle h(\alpha)\rangle = \frac{1}{x}\sum_{i=1}^{x} \int dt\, \delta(c_i(t),\alpha) \qquad x = 4, 5 \qquad (2)$$

in $KC_{24}(NH_3)_4$ and $KC_{24}(NH_3)_5$. $\langle h(\alpha)\rangle$ spans the range $(-\pi/2, \pi/2)$, corresponding to the vector connecting the selected H atom to the average position of the three H atoms belonging to the same molecule ranging from antiparallel to parallel with respect to the $t = 0$ orientation. Assuming an NH_3 molecule to be in its ideal geometry, the absence of a spinning motion around the C_3-axis would be characterized by a main band in $\langle h(\alpha)\rangle$ not wider than 120°, corresponding to the selected H atom oscillating within one minimum of the rotational potential. On the contrary, for unhindered rotation about the C_3-axis $\langle h(\alpha)\rangle$ would span uniformly the whole range of angles. We found that NH_3 rotation is prevented (or strongly hindered) in $KC_{24}(NH_3)_5$, while it is much more likely to occur in $KC_{24}(NH_3)_4$ at both low and high temperature. This result may support our finding that the redistribution of kinetic energy between the translational motion of the cation and degrees of freedom of NH_3 molecules (including rotation around C_3) is indeed more efficient in $KC_{24}(NH_3)_4$ than in $KC_{24}(NH_3)_5$, and is not very much dependent on the temperature of the simulation. No definitive conclusion can be drawn, on the basis of our simulations, as to whether C_3 rotation does indeed take place via hindered tunneling rotation[13] in $KC_{24}(NH_3)_4$, though we find that this mechanism need not strictly be invoked to explain the rotational motion of the NH_3 molecules in $KC_{24}(NH_3)_4$.

V. Summary and Conclusion

Geometry optimizations and FPMD simulations have been performed on a number of stage-I potassium and potassium-

ammonia GICs. In the unammoniated species, the preferred adsorption position for K is in a hollow site, in analogy with the K adsorption on a graphite surface.[28] Dependent on the interlayer separation, K in KC_{24} may be located midway between the two carbon layers (as also happens in KC_8) or it may be closer to one layer, at a distance very similar to the C−K separation in the graphite surface adsorption.

Inclusion of up to three ammonia molecules results in a displacement of K away from its hollow site, typically toward an on-top one. When 4 ammonia molecules are intercalated, $K(NH_3)_4^+$ symmetric square-pyramidal clusters are formed, with K again located above the center of a C ring. The N atoms are exactly in the mid-plane, while K is displaced toward one carbon plane. Intercalation of additional ammonia molecules affects the symmetry of the $K(NH_3)_4^+$ clusters as well as the optimized position of K, which is forced to move away from the hollow site.

Finite-temperature simulations were performed on KC_8, KC_{24}, $KC_{24}(NH_3)_4$, and $KC_{24}(NH_3)_5$ in the temperature range 373−573 K and simulation times 2−4 ps. Vertical oscillations of K were observed in all systems, with frequencies determined by the interlayer separation and independent of the composition of the intercalant. Thus, K is typically not associated with one single carbon layer, but rather it finds itself in turn closer to one or the other graphite sheet, and it frequently crosses the mid-plane. In addition, K is oscillating about its adsorption site in KC_8 at 373 K and diffusing in the *xy*-plane in KC_8 at 573 K and in all the other systems. The presence of ammonia molecules hinders free diffusion of K and modifies the amplitude of its oscillations perpendicular to the carbon planes, a reduction from ∼1 to ∼0.5 Å being observed as x increases from 4 to 5. This has important implications for understanding the role of intercalated NH_3 in the metal-non metal transition observed between $x = 4$ and $x = 4.5$, though longer simulation times would be required to draw definitive conclusions. Ammonia molecules were found to have their C_3-axis tilted with respect to the *ab*-plane of, on average, 8−13°, though large fluctuations were measured, determined by the vertical motion of K. These values agree favorably with the experimental estimate.[13] Finally, we found that NH_3 molecules do undergo rotation about their C_3-axis in $KC_{24}(NH_3)_4$ (at 373 and 573 K), and, possibly, in $KC_{24}(NH_3)_5$. Invocation of a tunneling mechanism to allow for this kind of motion is thus found not to be strictly necessary, at least in the former species.

Acknowledgment. We thank P. Edwards and N. Skipper for useful discussion. L.B. is grateful to the Queen's College, Oxford, for the award of a Florey EPA Studentship. Computing facilities were provided by the Oxford Supercomputing Centre and the EPSRC UKCP grant.

References and Notes

(1) Greenwood, N. N.; Earnshaw, A. *Chemistry of the Elements*; Pergamon: Oxford, 1984.
(2) DiVincenzo, D. P.; Rabii, S. *Phys. Rev. B* **1982**, *25*, 4110.
(3) Ashcroft, N. W.; Mermin, N. D. *Solid State Physics*; Saunders College, 1976.
(4) Harrison, W. A. *Electronic Structure and the Properties of Solids*; Dover: New York, 1989.
(5) Holzwarth, N. A. W.; Louie, S. G.; Rabii, S. *Phys. Rev. B* **1983**, *28*, 1013.
(6) Dresselhaus, M. S.; Dresselhaus, G. *Adv. Phys.* **1981**, *30*, 139.
(7) York, B. R.; Solin, S. A. *Phys. Rev. B* **1985**, *31*, 8206.
(8) Qian, X. W.; Stump, D. R.; Solin, S. A. *Phys. Rev. B* **1986**, *33*, 5756.
(9) Fan, Y. B.; Solin, S. A.; Neumann, D. A.; Zabel, H.; Rush, J. J. *Phys. Rev. B* **1987**, *36*, 3386.
(10) Solin, S. A.; Zabel, H. *Adv. Phys.* **1988**, *37*, 87.
(11) Solin, S. A.; Huang, Y. Y. *Synth. Met.* **1988**, *23*, 223.
(12) Hark, S. K.; York, B. R.; Mahanti, S. D.; Solin, S. A. *Solid State Commun.* **1984**, *50*, 545.
(13) Walters, J. K.; Skipper, N. T.; Soper, A. K. *Chem. Phys. Lett.* **1999**, *300*, 444.
(14) Carlile, C. J.; Jaime, I. McL.; Lockhart, G.; White, J. W. *Mol. Phys.* **1992**, *76*, 173.
(15) Solin, S. A. *J. Phys. IV* **1991**, *1*, 311.
(16) Zhang, J. M.; Eklund, P. C.; Fan, Y. B.; Solin, S. A. *J. Phys. IV* **1991**, *1*, 311.
(17) Jortner, J. *J. Chem. Phys.* **1959**, *30*, 389.
(18) Huang, H. H.; Fan, Y. B.; Solin, S. A.; Zhang, J. M.; Eklund, P. C.; Heremans, J.; Tibetts G. G. *Solid State Commun.* **1987**, *64*, 443.
(19) Parr, R. G.; Yang, W. *Density Functional Theory of Atoms and Molecules*; Oxford University Press: Oxford, 1989.
(20) McKie, D.; McKie, C. *Essentials of Crystallography*; Blackwell Scientific: Oxford, 1986.
(21) Doll, G. L.; Yang, M. H.; Eklund, P. C. *Phys. Rev. B* **1987**, *35*, 9790.
(22) Remler, D. K.; Madden, P. A. *Mol. Phys.* **1990**, *70*, 921.
(23) Payne, M. C.; Teter, M. P.; Allan, D. C.; Arias, T. A.; Joannopoulos, J. D. *Rev. Mod. Phys.* **1992**, *64*, 1045.
(24) We used the codes CASTEP 3.9 and CASTEP 4.2 academic versions, licensed under UKCP-MSI Agreement, 1999.
(25) Monkhorst, H. J.; Pack, J. D. *Phys. Rev. B* **1976**, *13*, 5188.
(26) Vanderbilt, D. *Phys. Rev. B* **1990**, *41*, 7892.
(27) Perdew J. P.; Wang, Y. *Phys. Rev. B* **1992**, *46*, 6671.
(28) Lou, L.; Österlund, L.; Hellsing, B. J. *Chem. Phys.* **2000**, *112*, 4788.
(29) The distance of 2.82 Å has been calculated[28] for the "condensed phase" of K on graphite, characterized by a local coverage $\theta = 1$. This system corresponds to the stoichiometry C_8K. The corresponding value for $\theta = 0.25$ is 2.77−2.79 Å. $C_{24}K$ would have a "coverage" intermediate between these two values.
(30) Österlund, L.; Chakarov, D. V.; Kasemo, B. *Surf. Sci.* **1999**, *420*, 174.
(31) Cui, J.; White, J. D.; Diehl, R. D.; Anette, J. F.; Cole, M. W. *Surf. Sci.* **1992**, *279*, 149.
(32) Barnard, J. C.; Hoch, R. H.; Palmer, R. E. *Surf. Sci.* **1993**, *287/288*, 178.
(33) In this way, the motion of K is "adiabatic" with respect to the faster moving NH_3 molecules.
(34) We computed the C_3 tilt angle from the position of the N atom and of the center of mass of the ammonia molecule. Due to the large distortions in the NH_3 ideal geometry during finite temperature simulations, the values obtained should be regarded as purely indicative.